The (in-)validity of the WSSUS Assumption in Vehicular Radio Channels

Laura Bernadó[1], Thomas Zemen[1], Fredrik Tufvesson[2], Andreas F. Molisch[3], Christoph F. Mecklenbräuker[4]

[1]Forschungszentrum Telekommunikation Wien (FTW), Vienna, Austria
[2]Department of Electrical and Information Technology, Lund University, Lund, Sweden
[3]Department of Electrical Engineering, University of Southern California, Los Angeles, CA, USA
[4]Institut of Telecommunications, Technische Universität Wien, Vienna, Austria
Contact: bernado@ftw.at

***Abstract*—The assumption of wide-sense-stationarity (WSS) and uncorrelated scattering (US) of wireless propagation channels is widespread for the design and analysis of wireless propagation channels. However, the assumption is only valid within a limited range. In this paper, we investigate the extension of this range not only in time (WSS), but also in frequency (US), for measured vehicular propagation channels. We do this by using the collinearity of the local scattering function, which is a bounded spectral distance metric, and thus allows us to set an indicative threshold, which in turn enables a WSS and a US test.**

We prove that the fading process in vehicular communications is strongly non-WSS, which agrees with results previously reported in the literature. Furthermore, for the first time (to the authors' knowledge), we show their non-US behavior as well, mainly in scenarios with rich scattering. The dimensions of the *minimum stationarity region* are on the order of 40 ms in time and 40 MHz in frequency.

I. Introduction

The wide-sense-stationary (WSS) uncorrelated-scattering (US) assumptions for wireless propagation channels imply that channel *statistics* (but not the channel realizations) are independent of time and center frequency. They allow a greatly simplified statistical description of channels, and - even more importantly - form the basis for many designs and analyses of wireless transceivers. However, the WSSUS assumptions are not always fulfilled in practice. They were introduced in [1] for ionospheric propagation channels; however, later work has shown them to be valid only for limited time-spans (WSS) and bandwidths (US) in cellular scenarios [2]. These limitations are particularly pronounced in vehicular, more precisely, vehicle-to-vehicle (V2V) propagation channels. When considering a non-stationary channel, the fading statistics have to be estimated as they change, both in time and in frequency. Therefore it is important to characterize for how long they can be considered to remain more or less constant.

A number of papers has investigated this topic in the past years, as the interest on vehicular communications has increased. A first definition of the stationarity time and stationarity bandwidth was proposed in [2], computed from the local scattering function (LSF) and the channel correlation function (CCF). It is a theoretical methodology derived for infinite time and frequency intervals, and is difficult to apply to measurements. There is also an increasing number of experimental contributions that are describing the non-stationarity of the vehicular channel in time, i.e. the non-WSS behavior. Ref. [3], [4], [5] measure the distance between locally defined power spectra of the fading process, and determine the range of validity of the WSS assumption. In [4], [5], the WSS assumption is characterized in terms of the stationarity distance, and longer distances are observed in presence of a strong line-of-sight component and in convoy measurements. Refs. [6], [7] define a statistical test based on the evolutionary spectrum of a signal estimated at different time instances. However, the US assumption has been tested far less - to the best of our knowledge, never in V2V channels, and even for vehicle-to-infrastructure channels only in a few cases (e.g., [8]).

In this paper we fill this gap. We present measures of the stationarity area in both time (WSS) and frequency (US) for V2V propagation channels. The evaluations are based on extensive measurements performed in a variety of environments. We compare the locally defined scattering function estimated from the measured channels to assess their stationarity in time and in frequency.

The paper is organized as follows. The collinearity in time and frequency as a tool for performing the WSS and the US test are introduced in Sec. II. They are used on channel measurements and their results are discussed in Sec. III. Based on those, we suggest a redefinition of the WSSUS region dimensions in Sec. IV. Final remarks and conclusions are given in Sec. V.

II. Stationarity Assessment

The basis of our assessment is the time-varying frequency response (transfer function) $H(t, f)$ of the "effective" propagation channel. It includes the effects of the physical channel and the transmitter and receiver filters of the channel sounder used in the measurements. We consider $H[m, q]$ to be the discrete frequency response, sampled as $H[m, q] = H(t_\mathrm{s}m, f_\mathrm{s}q)$, where $m \in \{0, \ldots, S-1\}$ represents time sampled at t_s,

This work has been funded by the FTW project NOWIRE funded by Vienna Science and Technology Fund (WWTF). Part of this work was supported by the COST Action 2100 and IC1004. The Competence Center FTW Forschungszentrum Telekommunikation Wien GmbH is funded within the program COMET - Competence Centers for Excellent Technologies by BMVIT, BMWA, and the City of Vienna. The COMET program is managed by the FFG.

with S being the total number of recorded snapshots, and $q \in \{0, \dots, Q-1\}$ denotes frequency, with Q being the number of measured frequency bins. The total measurement bandwidth is denoted by B and defines a frequency resolution of $f_\mathrm{s} = B/Q$.

In order to be able to describe the power spectrum of a non-WSSUS fading process, we first have to define a time-frequency region within which we assume the WSSUS properties to hold [2]. This WSSUS or stationarity region is defined by M samples in time and N samples in frequency.

Using a sliding window over the recorded frequency response, we estimate a time-frequency dependent scattering function by means of the discrete version of the local scattering function (LSF).

We estimate the LSF for consecutive stationarity regions in time and frequency indexed by (k_t, k_f) as in [2], [9] using a multitaper based estimator in order to obtain multiple independent spectral estimates from the same measurement and afterwards average them [10], [11]. The LSF estimate reads

$$\hat{\mathcal{C}}[k_t, k_f; n, p] = \frac{1}{IJ} \sum_{w=0}^{IJ-1} \left| \mathcal{H}^{(G_w)}[k_t, k_f; n, p] \right|^2, \quad (1)$$

where $n \in \{0, \dots, N-1\}$ denotes the delay index, and $p \in \{-M/2, \dots M/2-1\}$ the Doppler index, respectively. The LSF at k_t, k_f corresponds to the center value of the time-frequency stationarity region. The delay and Doppler shift resolutions are given by $\tau_\mathrm{s} = 1/(Nf_s)$ and $\nu_\mathrm{s} = 1/(Mt_s)$.

The windowed frequency response $\mathcal{H}^{(G_w)}$ is calculated as

$$\mathcal{H}^{(G_w)}[k_t, k_f; n, p] = \sum_{m'=-M/2}^{M/2-1} \sum_{q'=-N/2}^{N/2-1} H[m'-k_t, q'-k_f] G_w[m', q'] \mathrm{e}^{-\mathrm{j}2\pi(pm'-nq')}, \quad (2)$$

where the tapers $G_w[m', q']$ shall be well localized within the support region $[-M/2, M/2-1] \times [-N/2, N/2-1]$ and are chosen as the discrete prolate spheroidal sequences (DPSS) [3], [9]. The number of used tapers is $I = 3$ in the time domain and $J = 3$ in the frequency domain, set based on the results of [12].

The relative time index within each stationarity region is denoted by the variable $m' \in \{-M/2, \dots, M/2-1\}$, and the relative frequency index by $q' \in \{-N/2, \dots, N/2-1\}$. The relationship between the relative and absolute time index is given by $m = [(k_t - 1)\Delta_t + m'] + M$, where $k_t \in \{1 \dots \lfloor \frac{S-M}{\Delta_t} \rfloor\}$ and Δ_t denotes the time shift between consecutive stationarity regions. In the frequency domain the relationship is $q = [(k_f - 1)\Delta_f + q'] + N$, where $k_f \in \{1 \dots \lfloor \frac{Q-N}{\Delta_f} \rfloor\}$, and Δ_f denotes the frequency shift.

A. Collinearity of the LSF

Stochastic processes whose statistical properties do not change in time are considered WSS in time. Likewise, stationarity in frequency relates to the US property. For testing stationarity in both domains we use the locally defined power spectra of a fading process, i.e. the LSF described in the previous section.

For calculating the LSF we first assume a *minimum stationarity region*, and we are interested in investigating whether it can be enlarged. In order to do that, we need to test whether neighboring LSFs (shifted by Δk_t in time and Δk_f in frequency) are similar enough such that the fading process can be considered stationary.

To make precise the notion of "similar enough", we use a spectral distance metric called collinearity, introduced in [13]. The collinearity is a bounded metric $\gamma \in [0, 1]$ that compares the LSF at different time instances and frequency regions. A collinearity close to 1 is an outcome for very similar power spectra, whereas a collinearity close to 0 results from comparing two very dis-similar spectral densities.

We differentiate between the collinearity in the time and in the frequency domain, in order to test the WSS and US assumptions separately. Hence, the collinearity in time is defined as

$$\gamma_t[k_t, k_t + \Delta k_t] = \frac{\sum_{n=0}^{N-1} \sum_{p=-M/2}^{M/2-1} \sum_{k_f=-N/2}^{N/2-1} \hat{\mathcal{C}}[k_t, k_f; n, p] \odot \hat{\mathcal{C}}[k_t + \Delta k_t, k_f; n, p]}{\|\hat{\mathcal{C}}^{(k_t)}\|_2 \|\hat{\mathcal{C}}^{(k_t + \Delta k_t)}\|_2}, \quad (3)$$

where the L_2 norm $\| \cdot \|_2$ operates on $\hat{\mathcal{C}}^{(k_t)}$, which is the vectorized LSF at a given time instant k_t. Analogously, the collinearity in frequency reads

$$\gamma_f[k_f, k_f + \Delta k_f] = \frac{\sum_{n=0}^{N-1} \sum_{p=-M/2}^{M/2-1} \sum_{k_t=-M/2}^{M/2-1} \hat{\mathcal{C}}[k_t, k_f; n, p] \odot \hat{\mathcal{C}}[k_t, k_f + \Delta k_f; n, p]}{\|\hat{\mathcal{C}}^{(k_f)}\|_2 \|\hat{\mathcal{C}}^{(k_f + \Delta k_f)}\|_2}, \quad (4)$$

where now the L_2 norm operates on $\hat{\mathcal{C}}^{(k_f)}$, which is the vectorized LSF at a given center frequency k_f.

B. Stationarity Time and Stationarity Bandwidth

We define the *stationarity time* T_stat and the *stationarity bandwidth* F_stat, as those time (or frequency) ranges where the collinearity exceeds a threshold $\alpha_\mathrm{th} = 0.9$ [3]:

$$X_\mathrm{stat}[k_x] = \rho_x (D_x - \Delta_x) + \rho_x \Delta_x \left(\sum_{\Delta k_x = 1-k_x}^{K_x - k_x} \alpha[k_x, k_x + \Delta k_x] \right), \quad (5)$$

where x stands for either t to obtain the T_stat or f to obtain the F_stat. The resolution is denoted by ρ_x, with $\rho_t = t_s$, and $\rho_f = f_s$, and D_x stands for the dimension of the *minimum stationarity region* in time $D_t = M$ and in frequency $D_f = N$. The indicator function $\alpha[k, k + \Delta k]$ is defined as

$$\alpha[k, k + \Delta k] = \begin{cases} 1 & : \quad \gamma[k, k + \Delta k] > \alpha_\mathrm{th} \\ 0 & : \quad \text{otherwise.} \end{cases} \quad (6)$$

In order to avoid overestimated T_stat values due to considering regions with only noise, only time instances whose root mean square delay spread is greater than 0.5 ns are considered.

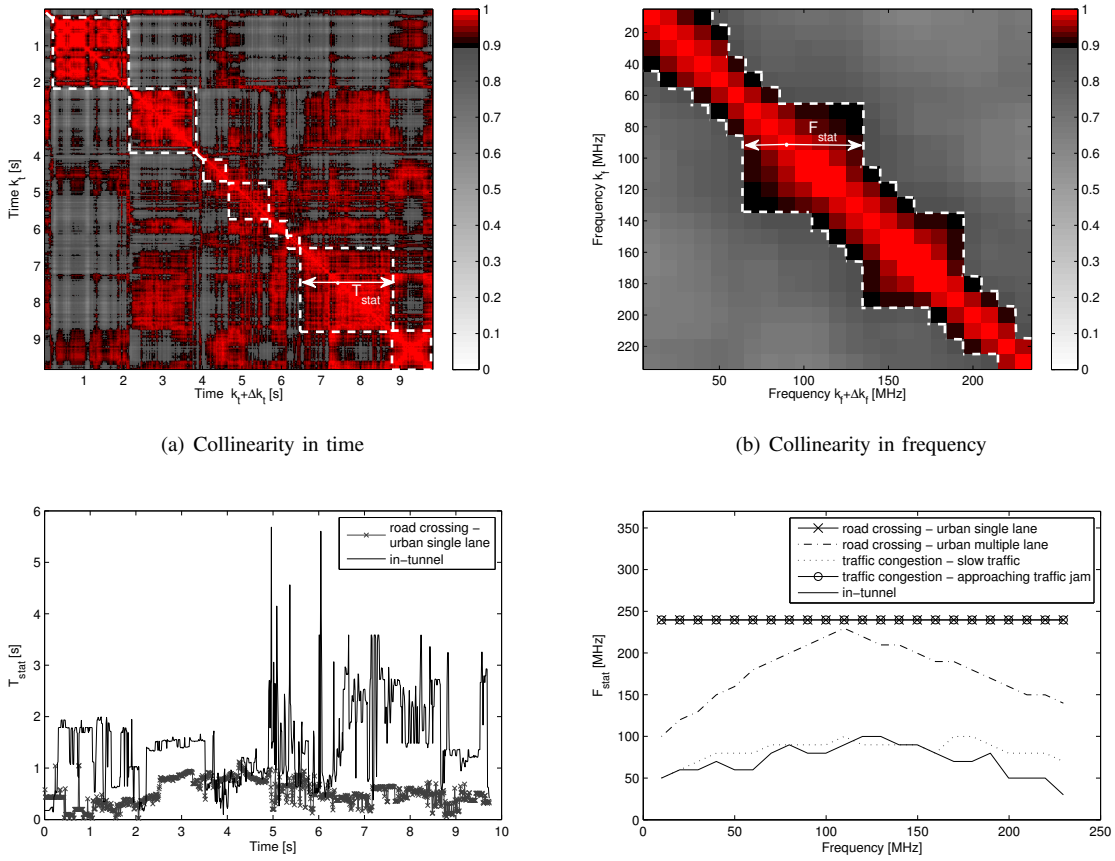

(a) Collinearity in time

(b) Collinearity in frequency

(c) Stationarity time

(d) Stationarity bandwidth

Fig. 1. Collinearity in time and frequency for in-tunnel measurement.

III. Validation of the WSS and US Assumptions on Measured Channels

For the analysis carried out in this paper, we use the channel frequency responses collected in a vehicular measurement campaign DRIVEWAY'09.

The measurements were carried out in six different scenarios: (i) *road-crossing*, (ii) *general line-of-sight obstruction* on a highway, (iii) *merging lanes* in a rural environment, (iv) *traffic congestion* situations, (v) *in-tunnel*, and (vi) *on-bridge*. Furthermore, we sub-classify the *road-crossing*, and the *traffic congestion* scenarios. Within the *road-crossing* we measured intersections in: (a) suburban environment with traffic, (b) suburban environment without traffic, (c) urban intersection between single lane streets, and (d) urban intersection between multiple lane streets. We performed measurements for the two most typical driving situations in a *traffic-congestion*: (a) when the transmitter and receiver cars are stuck in a traffic jam and they move slowly, and (b) when one of the cars is in the traffic jam and the other one approaches from behind at high speed.

A set of 3 to 13 measurement runs is recorded for each scenario. The recorded frequency responses $H[m, q]$ consist of $S = 32500$ or 65000 snapshots sampled at $t_s = 307.2\,\mu$s, resulting in a $10\,$s or $20\,$s duration run, depending on the measurement. The measurements were conducted using a carrier frequency of $5.6\,$GHz with a total bandwidth $B = 240\,$MHz in $Q = 769$ frequency bins. We employed a 4×4 multiple-input-multiple-output system, thus obtaining a total of $L = 16$ individual measured links. We used a 4-antenna element uniform linear array with directional patch vehicular antennas, radiating towards the front, back, right, and left with respect to the driving direction. More details regarding the measurements can be found in [14].

For the investigation presented in this paper, we are interested in testing the stationarity of the channel without considering angular information. Therefore, we do not consider the LSF of each individual link, and in order to resemble an omnidirectional antenna radiation pattern, we calculate the combined LSF for the $L = 16$ links as

$$\hat{\mathcal{C}}[k_t, k_f; n, p] = \frac{1}{L} \sum_{l=1}^{L} \hat{\mathcal{C}}^{(l)}[k_t, k_f; n, p], \tag{7}$$

where $\hat{\mathcal{C}}^{(l)}[k_t, k_f; n, p]$ is the LSF estimated for each individual link l as in Eq. (1).

We estimate the LSF using the *minimum stationarity region* of dimensions $M = 64$ samples corresponding to $19.66\,$ms and $N = 64$ samples corresponding to $19.97\,$Hz. We select

the sliding shift to be half of the *minimum stationarity region* dimension, i.e. $\Delta_t = 32$ samples in the time domain and $\Delta_f = 32$ samples in the frequency domain, resulting in a resolution of $9.65\,\text{ms}$ in T_{stat} and of $9.99\,\text{MHz}$ in F_{stat}.

We show in Fig. 1 (a) and (b) the collinearity in time and frequency for an *in-tunnel* measurement, where we highlight the threshold $\alpha_{\text{th}} = 0.9$ using the color coding reported on the right hand side of each figure. The result of applying the aforementioned threshold to both collinearities is shown in subfigures (c) and (d).

The stationarity time T_{stat} is plotted as a function of time in the subfigure 1 (c). We observe that T_{stat} shows strong variations. This is caused by the small number of samples in the time domain used for estimating the LSF in comparison to the total measurement time.

Nevertheless, we expect a smoother curve. The T_{stat} indicates for how long the fading process remains stationary in time, therefore we expect that the T_{stat} obtained for a given time instance is constant in time exactly for a period of duration T_{stat}. For instance, in Fig. 1 (c), at $1\,\text{s}$, the $T_{\text{stat}} = 1.8\,\text{s}$, which means that the process remains stationary for $1.8\,\text{s}$ about the time $1\,\text{s}$. Based on that, we expect that all neighboring time instances within a period of length $1.8\,\text{s}$ have a $T_{\text{stat}} = 1.8\,\text{s}$, i.e. we expect a flat line at $1.8\,\text{s}$. We show this "expected" T_{stat} value on Fig. 1 (a) with a white trace.

On the other hand, it is very easy to identify the region limited by the threshold on the collinearity in frequency, in Fig. 1 (b). The resulting stationarity bandwidth is plotted as a function of frequency in Fig. 1 (d). Here, the results are smoother since the ratio between the stationarity region length in frequency and the total bandwidth is large enough.

Furthermore, we show the stationarity time for a *road crossing* measurement performed in an urban single lane intersection with cross markers in Fig. 1 (c). Noteworthy are the low values of T_{stat} observed in the crossing scenario, namely below $1\,\text{s}$.

Likewise, we plot the F_{stat} for four more scenarios in Fig. 1 (d). Here it is remarkable that the F_{stat} encompasses the whole measurement bandwidth in some of the scenarios, such as for the *road crossing in an urban single lane intersection* measurement, and for the approaching *traffic congestion* measurement.

In other cases, such as in the *road crossing* measurement, performed in an *urban multiple lane intersection*, in the *traffic congestion* with slow traffic, and in the *in-tunnel* measurement, $F_{\text{stat}} < B$. It is noteworthy that there is a rich scattering environment for all the scenarios where the US property does not hold over the whole measurement bandwidth.

Furthermore, we observe a decrease of F_{stat} at low and high frequencies. This is due to the band limited measurements, observable as an edge effect in the collinearity plot in Fig. 1 (b).

Moreover, we want to point out that there is no direct relationship between stationarity time and stationarity bandwidth. For instance, a process can have a long stationarity time but small stationarity bandwidth, such as observed in the *road crossing* in an urban single lane intersection.

TABLE I
MINIMUM OBSERVED STATIONARITY TIME T_{STAT} AND STATIONARITY BANDWIDTH F_{STAT} USING $M = 64 = 19.66\,\text{MS}$ AND $N = 64 = 19.97\,\text{HZ}$

Stationarity region dimensions		T_{stat}	F_{stat}
Road crossing - suburban with traffic *(3 measurements)*	min:	29.49 ms	189.76 MHz
	5% out:	69.69 ms	229.76 MHz
	mean:	1.38 s	237.69 MHz
	std:	0.91 s	8.71 MHz
Road crossing - suburban without traffic *(11 measurements)*	min:	49.15 ms	59.93 MHz
	5% out:	266.04 ms	199.69 MHz
	mean:	1.75 s	232.94 MHz
	std:	0.92 s	25.55 MHz
Road crossing - urban single lane *(5 measurements)*	min:	19.66 ms	159.80 MHz
	5% out:	98.67 ms	219.76 MHz
	mean:	0.49 s	236.91 MHz
	std:	0.25 s	10.46 MHz
Road crossing - urban multiple lane *(5 measurements)*	min:	29.49 ms	29.96 MHz
	5% out:	77.77 ms	50.00 MHz
	mean:	0.61 s	159.01 MHz
	std:	0.47 s	62.69 MHz
General LOS obstruction - Highway *(12 measurements)*	min:	19.66 ms	39.95 MHz
	5% out:	196.99 ms	69.81 MHz
	mean:	2.16 s	199.96 MHz
	std:	1.12 s	62.73 MHz
Merging lanes - rural *(7 measurements)*	min:	19.66 ms	$\geq$ 239.69 MHz
	5% out:	509.93 ms	$\geq$ 239.69 MHz
	mean:	2.59 s	$\geq$ 239.69 MHz
	std:	0.81 s	$\geq$ 0 MHz
Traffic congestion - slow traffic *(11 measurements)*	min:	39.32 ms	29.96 MHz
	5% out:	245.09 ms	79.98 MHz
	mean:	1.71 s	174.80 MHz
	std:	0.99 s	65.52 MHz
Traffic congestion - approaching traffic jam *(7 measurements)*	min:	68.81 ms	59.93 MHz
	5% out:	225.63 ms	109.81 MHz
	mean:	1.79 s	215.00 MHz
	std:	10.7 s	46.60 MHz
In-tunnel *(7 measurements)*	min:	29.49 ms	19.97 MHz
	5% out:	167.62 ms	39.92 MHz
	mean:	1.06 s	80.34 MHz
	std:	0.93 s	39.53 MHz
On-bridge *(4 measurements)*	min:	19.66 ms	109.86 MHz
	5% out:	924.19 ms	129.79 MHz
	mean:	2.64 s	221.67 MHz
	std:	0.68 s	35.48 MHz

IV. DEFINITION OF THE MINIMUM STATIONARITY REGION DIMENSIONS

Until now, we have only shown results for single measurement runs in different scenarios. Nevertheless we have at our disposal a large set of measurements [14]. We next compute the minimum T_{stat} and F_{stat} for the overall measurement set, and how often these minima are obtained. These results can also be used to possibly enlarge the *minimum stationarity region*.

Table I lists, for each scenario: (i) the minimum T_{stat} and F_{stat} (ii) the 5% outage probability, which indicates the dimension such that in 95% of all cases, the stationarity region is larger than this particular value, (iii) the mean value, and (iv) the standard deviation of T_{stat} and F_{stat}.

We point out that the minimum T_{stat} in all scenarios is relatively low, confirming previous reports [4], [3], [9].

The shortest stationarity bandwidth obtained reaches the extension of the *minimum stationarity region*. From the values in Tab. I, we find that the smallest stationarity bandwidth occurs in the *road crossing* in an urban intersection of multiple lane streets, *traffic congestion* with slow traffic, and *in-tunnel*. All of them have a rich scattering environment, as already noticed before. For the *in-tunnel* measurements, the fact that the reflections on the walls and ceiling cause multiple components stemming from the same scatterer at different delays, offers a physical explanation of the violation of the US condition.

We note that the standard deviation of F_{stat} for the *merging lanes* scenario in rural environment is $0\,\text{MHz}$, in all 7 measurement runs. The apparently stable result, $F_{\text{stat}} = B$, is due to the limited measurement bandwidth B.

Note that the straight curves in Fig. 1 (d) for *road crossing* in an urban single lane intersection, and for the *traffic congestion* with an approaching traffic jam situation correspond to the stationarity bandwidth obtained for a single measurement run, whereas the results listed in Tab. I are obtained from the whole data ensemble. This is why the mean value of the stationarity bandwidth for these two scenarios is not $240\,\text{MHz}$, as in Fig. 1 (d).

We observe that the mean stationarity bandwidths of all measurements except for the *in-tunnel* measurement are above 150 MHz. This is very much larger than the required $10\,\text{MHz}$ communication bandwidth of an IEEE 802.11p system.

Based on the results above, the size of the minimum stationarity region (window used for analysis) can be doubled, yielding better resolution. We show the T_{stat} and the F_{stat} for the *in-tunnel* measurement in Fig. 2 (a) and (b) in gray dashed line using the doubled stationarity region extension, and compare it to the initial choice in black solid line.

V. Conclusions

In this contribution we extended the use of the collinearity for testing both the wide-sense stationarity (WSS) and the uncorrelated-scattering (US) assumptions on measured vehicle-to-vehicle (V2V) channels. We applied the collinearity in time and in frequency over the local scattering function (LSF). We set an indicative threshold on this bounded metric over which we consider the observed process to be stationary either in time or in frequency, and based on it defined the stationarity time T_{stat} and the stationarity bandwidth F_{stat}.

We presented evaluations of extensive measurements of V2V propagation channels in a large variety of scenarios. Based on the obtained results for T_{stat} and F_{stat}, we conclude that the *minimum stationarity region* length used for estimating the LSF is approximately $40\,\text{ms}$ and $40\,\text{MHz}$.

It is therefore safe to conclude that violations of the US assumption are not observable within the $10\,\text{MHz}$ bandwidth of an IEEE 802.11p system. However, violations of the WSS assumption are relevant to IEEE 802.11p systems because the frame duration may exceed the stationarity time.

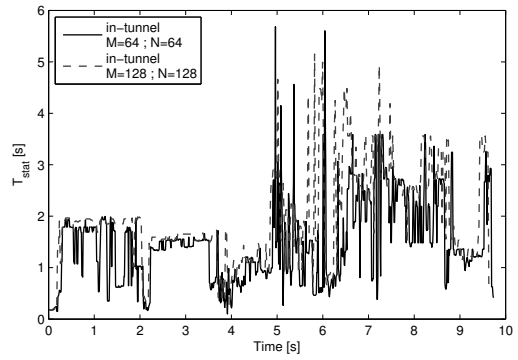

(a) Stationarity time

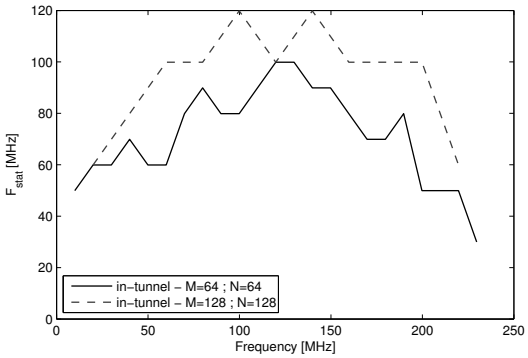

(b) Stationarity bandwidth

Fig. 2. T_{stat} and F_{stat} for an *in-tunnel* measurement using two sizes for the *minimum stationarity region*.

Furthermore, the obtained results indicate that violations of the WSS assumption do not necessarily imply violations of the US assumption.

References

[1] P. A. Bello, "Characterization of randomly time-variant linear channels," *IEEE Transactions on Communications*, vol. 11, pp. 360–393, 1963.

[2] G. Matz, "On non-WSSUS wireless fading channels," *Wireless Communications, IEEE Transactions on*, vol. 4, no. 5, pp. 2465–2478, September 2005.

[3] A. Paier, T. Zemen, L. Bernadó, G. Matz, J. Karedal, N. Czink, C. Dumard, F. Tufvesson, A. F. Molisch, and C. F. Mecklenbräuker, "Non-WSSUS vehicular channel characterization in highway and urban scenarios at 5.2 GHz using the local scattering function," in *Smart Antennas, 2008. WSA 2008. International ITG Workshop on*, February 2008, pp. 9–15.

[4] O. Renaudin, V.-M. Kolmonen, P. Vainikainen, and C. Oestges, "Non-stationary narrowband MIMO inter-vehicle channel characterization in the 5-GHz band," *Vehicular Technology, IEEE Transactions on*, vol. 59, no. 4, pp. 2007–2015, May 2010.

[5] A. Ispas, G. Ascheid, C. Schneider, and R. Thomä, "Analysis of local quasi-stationarity regions in an urban macrocell scenario," in *Vehicular Technology Conference (VTC 2010-Spring), 2010 IEEE 71st*, may 2010, pp. 1 –5.

[6] T. Willink, "Wide-sense stationarity of mobile MIMO radio channels," *Vehicular Technology, IEEE Transactions on*, vol. 57, no. 2, pp. 704 –714, march 2008.

[7] D. Umansky and M. Patzold, "Stationarity test for wireless communication channels," in *Global Telecommunications Conference, 2009. GLOBECOM 2009. IEEE*, 30 2009-dec. 4 2009, pp. 1 –6.

[8] U. Chude-Okonkwo, R. Ngah, and T. Abd Rahman, "Time-scale domain characterization of non-WSSUS wideband channels," *EURASIP Journal on Advances in Signal Processing*, vol. 2011, no. 1, p. 123, 2011.

[9] L. Bernadó, T. Zemen, A. Paier, G. Matz, J. Karedal, N. Czink, F. Tufvesson, M. Hagenauer, A. F. Molisch, and C. F. Mecklenbräuker, "Non-WSSUS Vehicular Channel Characterization at 5.2 GHz - Spectral Divergence and Time-Variant Coherence Parameters," in *Assembly of the International Union of Radio Science (URSI)*, aug 2008, pp. 9–15.

[10] D. Percival and A. Walden, *Spectral analysis for physical applications: multitaper and conventional univariate techniques*, ser. Spectral Analysis for Physical Applications: Multitaper and Conventional Univariate Techniques. Cambridge University Press, 1993.

[11] D. Thomson, "Spectrum estimation and harmonic analysis," *Proceedings of the IEEE*, vol. 70, no. 9, pp. 1055–1096, September 1982.

[12] L. Bernadó, T. Zemen, A. Paier, J. Karedal, and B. H. Fleury, "Parametrization of the Local Scattering Function Estimator for Vehicular-to-Vehicular Channels," in *IEEE 70th Vehicular Technology Conference*, Anchorage, Alaska, USA, September 2009.

[13] M. Herdin, N. Czink, H. Ozcelik, and E. Bonek, "Correlation matrix distance, a meaningful measure for evaluation of non-stationary MIMO channels," in *Vehicular Technology Conference, 2005. VTC 2005-Spring. 2005 IEEE 61st*, vol. 1, May-June 2005, pp. 136–140.

[14] A. Paier, L. Bernadó, J. Karedal, O. Klemp, and A. Kwoczek, "Overview of Vehicle-to-Vehicle Radio Channel Measurements for Collision Avoidance Applications," in *IEEE 71st Vehicular Technology Conference,*, Taipei, Taiwan, May 2010.